LIQUID–LIQUID PHASE SEPARATION IN MULTICOMPONENT POLYMER SYSTEMS: INFLUENCE OF MOLAR-MASS DISTRIBUTION ON SHADOW CURVE AND PHASE-VOLUME RATIO*

Ron KONINGSVELD[a] and Karel ŠOLC[b]

[a] *Laboratory of Polymer Research, Katholieke Universiteit, Leuven, Belgium*
[b] *Michigan Molecular Institute, Midland, MI 48640, U.S.A.*

Received May 4, 1993
Accepted May 18, 1993

Dedicated to Professor Otto Wichterle on the occasion of his 80th birthday.

The effect of the molar-mass distribution (MMD), in particular the effect of a few higher molar-mass averages, on liquid–liquid phase behavior is studied with the aid of data based on the Flory–Huggins–Staverman model. The critical concentration and the critical slopes of the cloud-point curve and the shadow curve appear to be quite sensitive to m_z and m_{z+1}, and, theoretically, they could serve as a unique data source for estimating these averages. In practice, however, experimental difficulties and errors encountered, especially with the shadow-curve slope determination, are probably too great for these data to be of any use. Next, the entire cloud-point and shadow curves, and phase-volume ratios are examined with respect to the possible use to supply information on the MMD. At constant weight- and number-average molar mass, the cloud-point curve does not appear to be overly sensitive to the M_z-average in the studied range. As to the other curves, no simple relationship evolves either, higher averages *and* details of the MMD both determining shape and location of shadow and phase-volume curves. An alternative procedure is suggested which consists of fitting a set of delta functions to a series of data points.

The higher averages of a molar-mass distribution (MMD), such as the centrifuge averages M_z and M_{z+1}, are notoriously difficult to assess. The obvious absolute method is provided by the evaluation of sedimentation-diffusion equilibria in the ultracentrifuge, preferably under Θ-conditions. However, the procedure is so time-consuming that, but for a few studies in the past[1–6], virtually no application of the method can be found in literature. Usually, size-exclusion chromatography (GPC) is the source of information on the MMD, and values for higher averages, thus obtained, are often reported. Unfor-

* Part XXV in the series Liquid–Liquid Phase Separation in Multicomponent Polymer Systems; Part XXIV: Ber. Bunsenges. Phys. Chem. *89*, 1234 (1985).

tunately, such values are very uncertain because they are determined mainly by the amount of high molar-mass material in the sample which cannot be estimated very well by GPC. The higher averages being important, e.g., in theories of the rheology of polymer melts[7], consideration of a possible alternative should be worthwhile.

Some years ago it was demonstrated that the MMD markedly influences liquid–liquid phase relationships in polymer solutions[8 - 12]. It was also established that the higher-average molar masses play a predominant role here. This observation gave rise to an attempt at making use of this sensitivity and develop an alternative method for the determination of the MMD based on an analysis of phase relationships. Moderate success could be reported in that for a sample of polystyrene, MMD's derived from sedimentation–diffusion equilibrium and from coexisting phase compositions appeared to agree quite well[13]. The analysis was based on a quasi-binary phase diagram for solutions of this sample in cyclohexane which had been established earlier by Rehage et al. in an extensive experimental investigation[14]. These data, in conjunction with a good approximation of the Gibbs energy of mixing (ΔG) in its dependence on MMD, polymer concentration, ϕ, and temperature, T, allowed the sample's MMD to be estimated. Figure 1 shows the two MMD's which agree in range of molar masses covered ($10^5 - 10^6$), and in bimodal shape. The ultracentrifuge procedure was developed by Scholte[6].

The procedure has two drawbacks. In the first place, obtaining sufficiently accurate information on ΔG(MMD, ϕ, T) is time-consuming, and, secondly, the collection of a set of coexisting phase compositions is also a laborious affair. If a series of samples has to be analyzed the first disadvantage should not be too serious. Methods have been developed to determine the various parameters in the ΔG expression[15,16] and the investment in time would seem reasonable. The second problem might also be minimized if a fast procedure for the determination of equilibrium phase compositions could be developed.

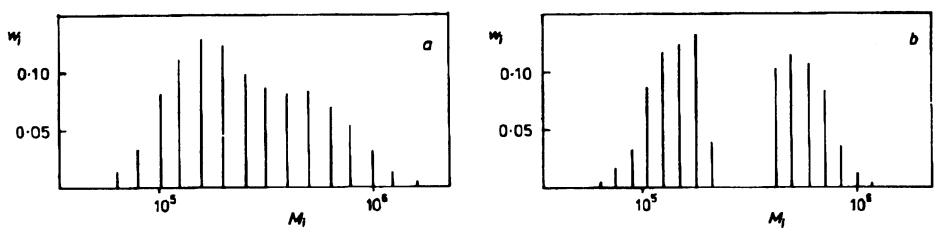

FIG. 1
Molar-mass distribution for a sample of polystyrene, obtained by sedimentation–diffusion equilibrium in the ultracentrifuge (*a*) and by analysis of liquid–liquid phase relations (*b*), both in cyclohexane

This paper is a preliminary report on an examination of possible simplifications in the data taking. In particular, we investigate whether either shadow curve or phase-volume ratio (as a function of temperature at a given initial polymer concentration) might offer useful tools in the assessment of the MMD, or of higher molar-mass averages. The analysis is theoretical, based on the ΔG expression derived independently by Staverman and Van Santen[17,18], Huggins[19,20] and Flory[21] (FHS model). However, the suggested procedure should be of general validity, because the equations used may easily be extended to cover systems in which the interaction function depends on the overall polymer concentration. Such an adaptation and its application to actual systems is currently being studied.

It should be mentioned that the first indication of possible viability of the approaches proposed here is contained in the early work by Boyer[22]. This author studied the volume of the concentrated phase at constant ϕ as a function of the composition of a binary solvent. The latter variable was used instead of temperature to effect a change in χ. Boyer claimed that the fashion in which the volume of the polymer-rich phase varies with the non-solvent concentration is indicative of the width of the initial MMD. It was shown later that Boyer's conclusion is indeed valid, albeit only if samples are compared in which the MMD is identical in type[23].

LIQUID–LIQUID PHASE RELATIONS IN QUASI-BINARY POLYMER SOLUTIONS

Owing to its inherent polydispersity with respect to chain length, no polymeric constituent can be treated as a single component. Consequently, a two-dimensional phase diagram for solutions of a polymer in a single solvent needs to be constructed and read with caution. In the present account, the scope will be limited to two-phase separations only. Such quasi-binary diagrams have characteristics illustrated schematically in Fig. 2 (refs[9 – 11,15,24,25]). We note that the liquid–liquid critical point cannot be identified with the extreme of the cloud-point curve (CPC). The dashed curve, called shadow curve,

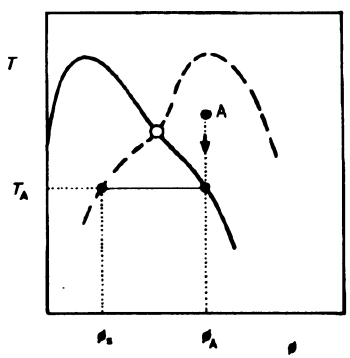

FIG. 2
Typical phase diagram for a quasi-binary polymer solution: —— cloud-point curve, - - - - shadow curve, O critical point

represents the overall polymer concentration of phases that are on the verge of appearing when a homogeneous solution like A is cooled down to the cloud point. Thus, the phase ϕ_s is in equilibrium with the bulk phase ϕ_A at the cloud-point temperature, T_A. The polymer in the bulk phase ϕ_A has the MMD of the initial polymer, whereas the MMD of the still infinitesimally small faction in the incipient shadow phase ϕ_s differs from that of the polymer in the bulk phase.

In the following we shall address the question to what extent the initial MMD exerts an influence on CPC and/or shadow curve when number- and weight-average molar mass are kept constant, but the higher averages vary. Measurement of the CPC is usual practice, but a shadow curve is less tractable experimentally. Instead of this elusive curve one might consider another property, more open to experimental determination. Measurement of the phase-volume ratio (to be denoted by r) is open to some degree of automatization[26 - 28] which might provide perspectives.

CALCULATION PROCEDURES

The FHS equation for solutions of a polydisperse polymer in a single solvent reads

$$\Delta G/NRT = \phi_0 \ln \phi_0 + \Sigma (\phi_i/m_i) \ln \phi_i + \chi\phi\phi_0 , \qquad (1)$$

where N is the total amount of lattice sites in moles, R is the gas constant, T is the absolute temperature, ϕ_0 and ϕ_i are the site fractions of solvent molecules and of polymer chains occupying m_i lattice sites each, respectively, χ is the Van–Laar interaction parameter, and $\phi = \Sigma \phi_i$ is the site fraction occupied by all polymer chains. Obviously, $\phi_0 = 1 - \phi$.

Equilibrium conditions are defined by the equality of chemical potentials μ_j. For the FHS expression we have

$$\Delta\mu_0/RT = \ln \phi_0 + (1 - m_n^{-1}) \phi + \chi\phi^2 \qquad (2a)$$

$$\Delta\mu_i/m_iRT = m_i^{-1} \ln \phi_i + m_i^{-1} - 1 + (1 - m_n^{-1}) \phi + \chi\phi_0^2 , \qquad (2b)$$

where the number-average chain length m_n is defined by

$$\phi/m_n = \Sigma \phi_i/m_i . \qquad (3)$$

The equilibrium state for a separation into two phases, a and b, is determined by the conditions

$$\Delta\mu_{0a} = \Delta\mu_{0b} ; \qquad \Delta\mu_{ia} = \Delta\mu_{ib} . \qquad (4)$$

Introduction of Eqs (*2a*) and (*2b*), followed by subtraction and rearrangement, yields

$$\phi_{ib}/\phi_{ia} = e^{\sigma m_i}, \tag{5}$$

where ϕ_{ia} and ϕ_{ib} are the site fractions of polymer component i in the two phases, and σ is defined by

$$\sigma = \ln(\phi_{0b}/\phi_{0a}) + 2\chi(\phi_b - \phi_a). \tag{6}$$

The temperature dependence of the interaction parameter χ may be represented by

$$\chi = \chi_s + h/T. \tag{7}$$

We discuss the problem in general terms here and do not need to specify χ_s and h. The temperature axis in the various graphs will be represented by χ.

Cloud-Point and Shadow Curves

Phase b may be considered to represent the bulk phase (no subscript) and phase a the shadow curve (subscript s). Equation (*5*) thus becomes

$$\phi_i/\phi_{is} = e^{\sigma m_i}. \tag{8}$$

If w_i is the weight fraction of macromolecules i in the original polymer we may write

$$\phi_i = \phi w_i \tag{9a}$$

and, by virtue of Eq. (*8*),

$$\phi_{is} = \phi w_i e^{-\sigma m_i}, \tag{9b}$$

so that the total polymer concentration in the shadow phase is

$$\phi_s = \phi \Sigma w_i e^{-\sigma m_i} \tag{9c}$$

and the number-average chain length of the polymer in the shadow phase, m_{ns}, is given by

$$\phi_s/m_{ns} = \phi \Sigma (w_i/m_i) e^{-\sigma m_i}. \tag{9d}$$

The calculation of a cloud point for a given MMD may proceed as follows. For any ϕ on the CPC there are two unknowns of direct physical interest, viz., ϕ_s and χ. The shadow concentration is determined by σ [Eq. (*9c*)] and, therefore, the choice of a trial value for σ ($\equiv \sigma_{in}$) is the first step in the calculation. Then, ϕ_s and m_{ns} can be computed

with Eqs (*9c*) and (*9d*). The equilibrium condition for the solvent, Eqs (*2a*) and (*4*), is now used to calculate χ which is then introduced into Eq. (*6*) to yield σ_{out}. The trial value σ_{in} is varied until $\Delta\sigma \equiv \sigma_{in} - \sigma_{out}$ is sufficiently close to zero to produce a meaningful solution. It should be noted that in multiphase systems there may be more than one solution (ϕ_s, χ, σ) for a chosen ϕ, corresponding to the formation of more than one incipient phase[11].

The location of the critical point on the CPC can be determined from Stockmayer's expression for critical state and spinodal[8]

$$\phi_c = [1 + (m_w/\xi)^{1/2}]^{-1} \qquad (10a)$$

$$\chi_c = [\phi_{0c}^{-1} + (\phi_c m_w)^{-1}]/2 , \qquad (10b)$$

where $\xi \equiv m_z/m_w$, and the weight- and z-averages are defined as usual

$$\phi m_w = \Sigma \phi_i m_i ; \qquad \phi m_w m_z = \Sigma \phi_i m_i^2 .$$

Furthermore[11], the slope of the CPC at the critical point is determined by m_w and ξ, too

$$(d\chi/d\phi)_c = [1 + (\xi/m_w)^{1/2}]^2 \, (1 - \xi^{-1})/2 , \qquad (10c)$$

whereas the slope of the shadow curve here is affected also by the (z + 1)st average

$$(d\chi/d\phi_s)_c = (d\chi/d\phi)_c \, (d\phi/d\phi_s)_c =$$

$$= -(d\chi/d\phi)_c \, (3 m_z + 2 m_z^{1/2} - m_{z+1})/(m_{z+1} + 2 m_z^{1/2} + 4 m_w - 3 m_z) . \qquad (10d)$$

It is interesting to note that while the CPC slope at the critical point is always positive [cf. Eq. (*10c*)], the shadow-curve slope $(d\chi/d\phi_s)_c$ can go either way. For "well behaved" distributions (probably the majority of cases) all multiplicative factors of Eq. (*10d*) are positive, yielding the slope $(d\chi/d\phi_s)_c$ negative as expected. However, if either of the parentheses in the numerator or denominator of Eq. (*10d*) becomes negative, the sign of the slope $(d\chi/d\phi_s)_c$ is switched to the positive.

Accordingly, there are two distinct conditions for having the shadow-curve slope > 0:

1) The derivative $(d\chi/d\phi_s)_c$ will be positive if the denominator of Eq. (*10d*) becomes negative, i.e., if

$$m_{z+1} < 3 m_z - 2 m_z^{1/2} - 4 m_w , \qquad (11a)$$

which can be further simplified for $m_v \to \infty$ (polymer with very high molecular weight) as

$$m_{z+1}/m_z < 3 - (4/\xi) . \qquad (11b)$$

Equation (*11b*) obviously demands that $\xi \equiv m_z/m_w$ be greater than 2. Similarly, the minimal permissible ξ can be formulated for the original full condition (*11a*) though the result is less transparent, available only in the form of an infinite series

$$\xi > 2 + (2/m_w)^{1/2} + 1/(2\,m_w) + 1/(2^7\,m_w^3)^{1/2} - \ldots . \qquad (11c)$$

Hence, it can be concluded that the positive slope $(d\chi/d\phi_s)_c$ of the "first kind" will only appear if the asymmetry is at least 2 (or somewhat higher if the weight average m_w is low), and if, at the same time, m_{z+1} is smaller than the R.H.S. of Eq. (*11a*). In qualitative terms, $(d\chi/d\phi_s)_c > 0$ requires a moderately high ratio m_z/m_w but relatively low ratio m_{z+1}/m_z, perhaps a somewhat unusual combination.

2) The derivative $(d\chi/d\phi_s)_c$ will be positive if the numerator of Eq. (*10d*) becomes negative, i.e., if

$$m_{z+1} > 3\,m_z + 2\,m_z^{1/2} . \qquad (11d)$$

This condition is recognized as the criterion for the so-called "unstable" critical points, i.e., critical points located on the unstable portion of the CPC between its two cusps[11], indicative of three-phase equilibria. Indeed, it has been known for some time from numerical studies of CPC's that in these cases the shadow curve develops a maximum and a minimum between which the slope flips its sign into positive[29]. However, since the focus of the present study is on two-phase separations, this case will not be pursued any further.

Fortunately there is no need for concern that both parenthese of Eq. (*10d*) might turn negative at the same time, with two negatives cancelling each other and restoring the original negative sign to the slope. Clearly, the conditions (*11a*) and (*11d*) are mutually exclusive.

Phase-Volume Ratio

The calculation of phase equilibria "within" the CPC is a little different. We fix ϕ and r, and derive the concentrations of the individual polymer components in each phase from the lever rule:

$$\phi_i\,(r+1) = r\,\phi_{ia} + \phi_{ib} , \qquad (12)$$

where $r \equiv V_a/V_b$ stands for the ratio of the volumes of phases a and b. Combining with Eq. (5), and summing over all polymer species, we get

$$\phi_b = (r+1)\,\phi\,\Sigma\, w_i/(1 + r\,e^{-\sigma m_i}) \tag{13a}$$

$$\phi_b/m_{nb} = (r+1)\,\phi\,\Sigma\, w_i/[m_i\,(1 + r\,e^{-\sigma m_i})] \tag{13b}$$

$$\phi_a = (r+1)\,\phi\,\Sigma\, w_i\,e^{-\sigma m_i}/(1 + r\,e^{-\sigma m_i}) \tag{13c}$$

$$\phi_a/m_{na} = (r+1)\,\phi\,\Sigma\, w_i\,e^{-\sigma m_i}/[m_i\,(1 + r\,e^{-\sigma m_i})]\,. \tag{13d}$$

A trial value for σ allows computation of all quantities defined in Eqs (*13*) and the calculation then proceeds as with the CPC.

Molar-Mass Distributions

Sets of Delta Functions

A binary set (w_1, m_1; w_2, m_2) is determined uniquely if three average molar masses are known, e.g., m_n, m_w and m_z. We have then four equations for the four unknowns

$$w_1 + w_2 = 1 \tag{14a}$$

$$m_n^{-1} = w_1/m_1 + w_2/m_2 \tag{14b}$$

$$m_w = w_1\,m_1 + w_2\,m_2 \tag{14c}$$

$$m_z\,m_w = w_1\,m_1^2 + w_2\,m_2^2\,. \tag{14d}$$

Sets with more than two components need additional assumptions. A quaternary set, for instance, has eight unknowns and could be constructed in the following fashion. Instead of two δ functions we use two sets 1 and 2, each containing two δ functions. We choose values for ν_1, ξ_1 and ν_2, ξ_2, where $\nu \equiv m_w/m_n$ and $\xi \equiv m_z/m_w$. Four unknowns remain, viz., the total weight fractions of sets 1 and 2 (w_1 and w_2) and their weight-average chain lengths m_{w1} and m_{w2}. The four equations (*14*) may be used in an adapted form

$$w_1 + w_2 = 1 \tag{15a}$$

$$m_n^{-1} = w_1 \nu_1 / m_{w1} + w_2 \nu_2 / m_{w2} \tag{15b}$$

$$m_w = w_1 m_{w1} + w_2 m_{w2} \tag{15c}$$

$$m_z m_w = w_1 \xi_1 m_{w1}^2 + w_2 \xi_2 m_{w2}^2 . \tag{15d}$$

Next, each set is subjected to the construction of a binary set with Eqs (*14*). The equations are solved numerically. Extension to 2^n components is conceivable in this manner.

Continuous Distributions

We select the exponential distribution (Schulz–Zimm distribution) to represent the MMD $w(m)$, and use it in the following form

$$w(m) = A\, m^{\lambda+1} e^{-\tau m} , \tag{16}$$

where A is the normalization factor, and λ and τ are parameters. Using the general equation for the integral between 0 and ∞,

$$\int_0^\infty m^{\lambda+n} e^{-\tau m} dm = \Gamma(\lambda + 1 + n)\, \tau^{-(\lambda+1+n)} \tag{17}$$

and the difference formula $\Gamma(p + 1) = p\Gamma(p)$, where $\Gamma(p)$ is the gamma function, it is easily shown that the three parameters are fixed by

$$A = W \tau^{\lambda+2} / \Gamma(\lambda + 2) , \qquad m_w = (\lambda + 2)/\tau , \qquad m_n = (\lambda + 1)/\tau , \tag{17a}$$

where the total mass W of polymer equals 1. Note that for an exponential distribution $\xi = 2 - \nu^{-1}$, i.e, its asymmetry, never greater than 2, is determined by its width ν.

Independent choice of ν and ξ desirable for modelling purposes is possible for an MMD represented by a sum of two exponential distributions

$$w(m) = A_1 m^{\lambda_1+1} e^{-\tau_1 m} + A_2 m^{\lambda_2+1} e^{-\tau_2 m} \tag{18}$$

and the construction described above in relation to Eqs (*15*) may be used to adapt the parameters to the actual values of m_n, m_w and m_z. The normalization factors A_1 and A_2

now refer to the relative masses of the two MMD's, listed as w_1 and w_2 in Table III. In calculating the CPC's and phase–volume ratios for continuous distributions, the summations in Eqs (*9c*), (*9d*) and (*13*) are replaced by integrations.

TABLE I
Parameters of MMD1's. Set of two δ functions

ξ:	1.5	2	3
w_1:	0.5	0.72361	0.86380
m_1:	29.29	38.20	43.84
w_2:	0.5	0.27639	0.13620
m_2:	170.7	261.8	456.2
m_{z+1}:	166.7	250.0	433.3
$(d\chi/d\phi_s)_c$:	−0.4579	−1.574	7.182

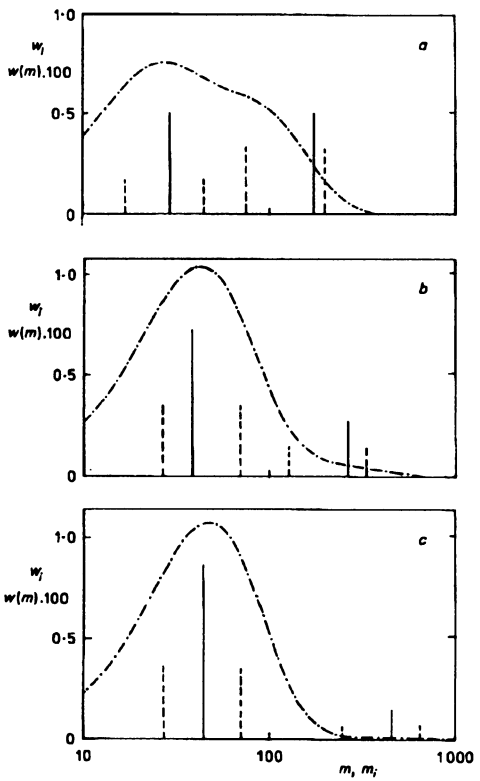

FIG. 3
Molar-mass distributions used in the calculations: —— set of two δ functions (MMD1), - - - - set of four δ functions (MMD2), - · - · - sum of two exponential distributions (MMD3). In all cases m_w = 100, ν = 2. Values for ξ: *a* 1.5, *b* 2, *c* 3

Distributions Used

The MMD's used in this study are shown in Figs 3*a* – 3*c*. They are all identical in m_w (= 100) and ν (= 2) but differ in asymmetries, $\xi \equiv m_z/m_w$, that vary as 1.5, 2, and 3, respectively, for figures *a* – *c*. Moreover, each figure of the triplet contains lines drawn

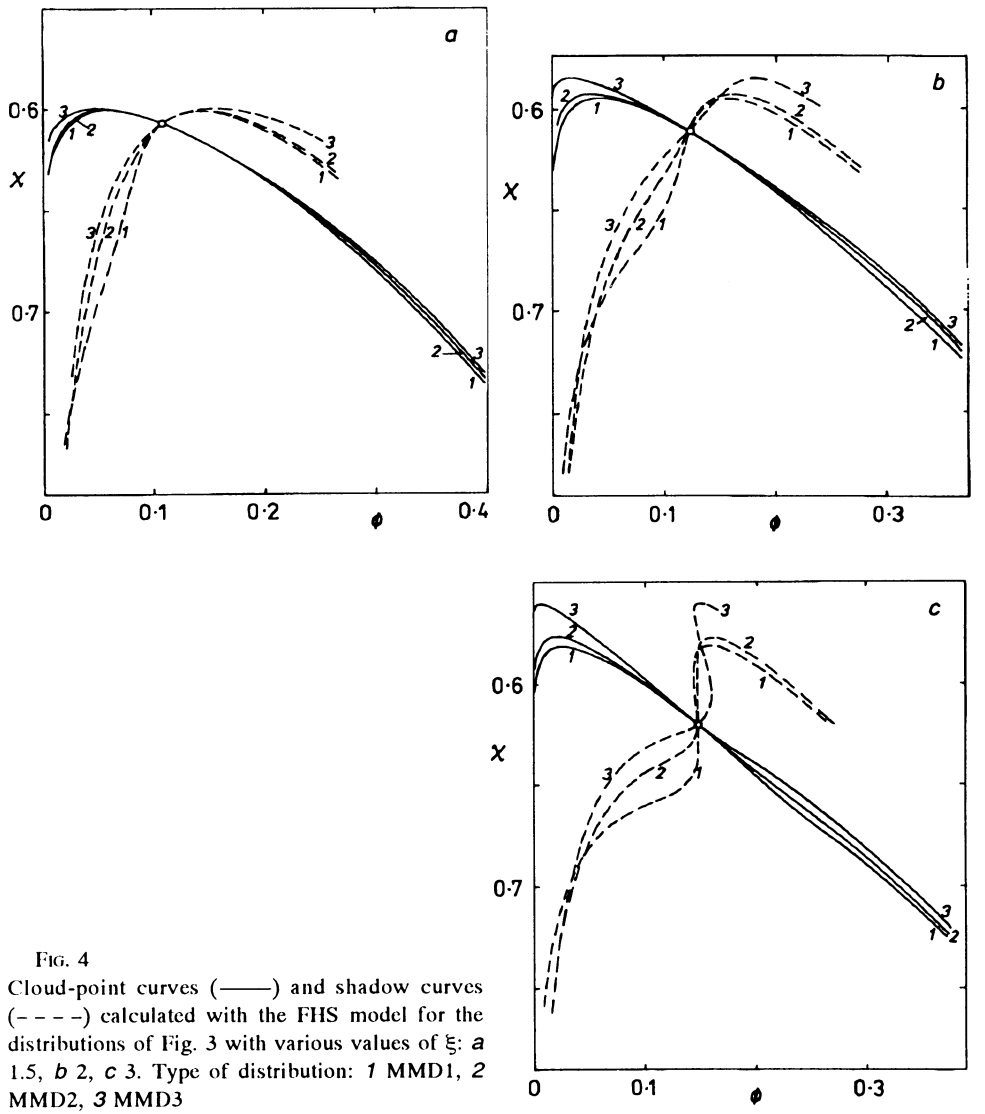

FIG. 4
Cloud-point curves (——) and shadow curves (- - - -) calculated with the FHS model for the distributions of Fig. 3 with various values of ξ: *a* 1.5, *b* 2, *c* 3. Type of distribution: *1* MMD1, *2* MMD2, *3* MMD3

in three different ways, corresponding to three types of distributions: MMD1 represents a binary polymer, MMD2 a quaternary one, and MMD3 is a sum of two exponential distributions. Various parameters of these distributions are listed in Tables I – III, each for one type of the distribution, with three numerical columns covering the three investigated asymmetries of 1.5, 2 and 3. We note that, plotted as the ordinate for MMD3 is simply $w(m)$ of Eq. (*18*), not 2.3 $m\,w(m)$ as normally required when employing logarithmic scale for m. Consequently, the area under the curve does not properly reflect the amounts of various fractions in the sample.

TABLE II
Parameters of MMD2's. Set of four δ functions; $\nu_1 = \nu_2 = 1.25$, $\xi_1 = \xi_2 = 1.2$

ξ:	1.5	2	3
w_1:	0.17094	0.35750	0.44365
m_1:	16.93	26.78	31.15
w_2:	0.17094	0.35750	0.44365
m_2:	44.33	70.12	81.55
w_3:	0.32906	0.14250	0.05635
m_3:	75.20	126.8	245.2
w_4:	0.32906	0.14250	0.05635
m_4:	196.9	331.9	642.1
m_{z+1}:	177.8	281.5	533.4
$(d\chi/d\phi_s)_c$:	−0.4091	−1.029	−2.706

TABLE III
Parameters of MMD3's. Set of two exponential functions; $\nu_1 = \nu_2 = 1.5$, $\xi_1 = \xi_2 = 4/3$, $\lambda_1 = \lambda_2 = 1$

ξ:	1.5	2	3
w_1:	0.78868	0.21132	0.06356
m_{w1}:	118.3	236.6	529.1
w_2:	0.21132	0.78868	0.93644
m_{w2}:	31.70	63.40	70.87
$\tau_1 \cdot 10^2$:	2.5359	1.2679	0.56697
$\tau_2 \cdot 10^2$:	9.4641	4.7321	4.2330
m_{z+1}:	194.4	333.4	722.2
$(d\chi/d\phi_s)_c$:	−0.3481	−0.5938	−0.3796

RESULTS

It follows from Eqs (*10a*) – (*10c*) and is confirmed by Figs 4*a* – 4*c* that, at constant m_w and m_z (i.e., in each figure of the triplet), the various MMD's share the same critical point as well as the same critical slope of the CPC. For the three different asymmetries ξ, the values of ϕ_c, χ_c and $(d\chi/d\phi)_c$ are 0.1091, 0.6071, 0.210 for Fig. 4*a*, 0.1239, 0.6111, 0.326 for Fig. 4*b*, and 0.1476, 0.6205, 0.459 for Fig. 4*c*, respectively. Thus, a 100% increase in m_z from 150 to 300 results in a more than 100% increase of the critical CPC slope, in a 35% growth of ϕ_c, and a 2.2% increase in χ_c. The lattermost, seemingly small, difference may still cause a sizeable change in critical temperature T_c. For instance, for a perfectly reasonable value of h in Eq. (*7*) of 100 K, and a T_c level of 300 K, the indicated difference in χ_c would amount to about 12 K in T_c.

On the other hand, the critical slope of the shadow curve is also affected by m_{z+1}. For the purpose of illustration, both m_{z+1} and $(d\chi/d\phi_s)_c$ (the latter computed from Eq. (*10d*)) are given in Tables I – III, too. Perhaps the best way to compare the effect of the MMD is to do so at constant m_w and m_z, i.e., within each of the Figs 4, and within the same column of Tables I – III. For the three columns in Tables I – III (i.e., in the sequence MMD1 – MMD3), the $(z + 1)$st average grows by the amounts of 17%, 33% and 67%, respectively. The negative shadow-curve slope, however, monotonously increases only for the first two columns ($\xi = 1.5$ and $\xi = 2$), with its absolute value dropping by 24% and 62% over MMD1–MMD3 range. The high positive slope $(d\chi/d\phi_s)_c$ for MMD1 with $\xi = 3$ (Table I, last column), confirmed by Fig. 4*c* (curve *1*), is an example of the positive slope of the first kind discussed above in the chapter "Cloud-Point and Shadow Curves". As expected, the criteria (*11a*) and (*11d*) are here satisfied. All shadow curves in Figs 4 are consistent with Eq. (*10d*), i.e., with slopes listed in Tables I – III.

Summarizing the above, the critical concentration ϕ_c and the slopes of both the CPC and the shadow curve appear to be quite sensitive to m_z and m_{z+1}, and their measurement is a possibility for distinguishing between various MMD's. In practice, however, it would be very time-consuming, with the experimental errors and difficulties probably too great (particularly in the case of the shadow curve) for these data to be of any use[10].

Turning now our attention to the entire curves, it is seen from Fig. 4*a* that at $\xi = 1.5$, the differences between various MMD's are small and probably hard to detect experimentally. The deviations increase when the value of ξ is increased. However, an unambiguous differentiation between, say, MMD3 of Fig. 4*b*, and MMD1 in Fig. 4*c* by only measuring the CPC would seem to be impossible. Type of the distribution and its ξ value both play their role and cannot be simply distinguished in the CPC's.

Using the phase-volume ratio to determine m_z and the type of distribution is bound to fail, too, as witnessed by Figs 5. Since usually the phase-volume ratio goes to zero at the cloud point if $\phi > \phi_c$, and to infinity for $\phi < \phi_c$, we show plots of χ against r as well as vs $1/r$. The different distributions show quite varied patterns which could be

used to extract information on the MMD. However, the m_z value should then be known. The higher concentrations (see ϕ = 0.2) appear to be useless altogether since the $\chi(r)$ curves do not differ a great for the three MMD's. Moreover, working with 20% polymer solutions would present experimental problems because of the high viscosity

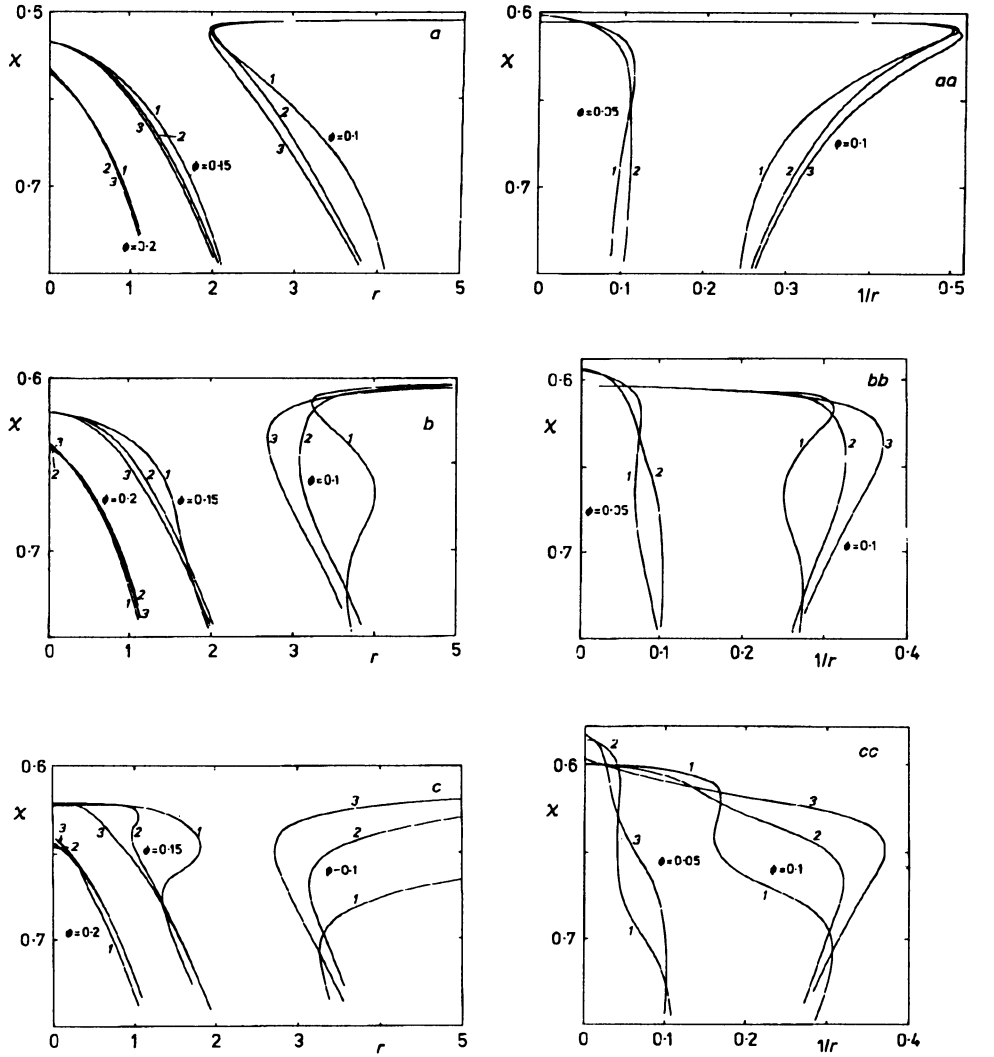

FIG. 5

Interaction parameter χ as a function of the phase-volume ratio, r, and $1/r$ for indicated values of the initial polymer concentration, ϕ (volume fraction), and for ξ 1.5 (*a*, *aa*), ξ 2 (*b*, *bb*), and ξ 3 (*c*, *cc*). Type of distribution: *1* MMD1, *2* MMD2, *3* MMD3

of such solutions. At relatively low concentrations ($\phi = 0.05$) the differences should be well detectable, but the phase-volume ratios involved are in the order 10 and difficult to assess. It is the middle range of concentrations, not far from ϕ_c, that would seem to be most useful since the different MMD's show up quite sensitively and well measurable in $\chi(r)$ behavior. Figure 6, redrawn from ref.[23], demonstrates that the calculated patterns can be confirmed by experiment.

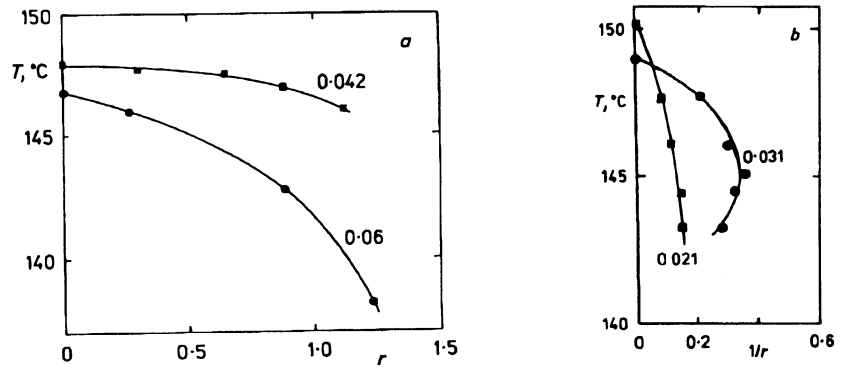

FIG. 6

Temperature as a function of phase-volume ratio (*a*) and $1/r$ (*b*) for indicated initial polymer concentrations (weight fraction). Polymer: linear polyethylene fraction with weight-average molar mass, M_w = 140 kg mol^{-1}, $\nu = 1.5$, $\xi = 1.9$. Solvent: diphenyl ether

It follows from the results of these calculations that, with the present experimental methods, a simple way of determining m_z does not exist. The same conclusion follows from similar calculations with other ν and ξ values. Therefore, we must conclude that procedures like those leading to Fig. 1 can hardly be avoided. In each of the two approaches indicated in the figure a wide grid of δ functions is introduced into a fitting procedure in which the data determine the weight fractions and the molar-mass range, occasionally rejecting specific values or ranges. The data of Fig. 6, and others, are currently being treated in this fashion.

We wish to thank M. Rozniak for technical help with some calculations and graphical work.

REFERENCES

1. Lansing W. D., Kraemer E. O.: J. Am. Chem. Soc. *57*, 1369 (1935).
2. Wales M., Williams J. W., Thompson J. O., Ewart R. H.: J. Phys. Colloid Chem. *52*, 983 (1948).
3. Williams J. W., Van Holde K. E., Baldwin R. L., Fujita H.: Chem. Rev. *58*, 715 (1958).

4. Fujita H.: *Mathematical Theory of Sedimentation Analysis*. Academic Press, New York 1962.
5. Scholte Th. G.: J. Polym. Sci., A2 *6*, 91, 111 (1968).
6. Scholte Th. G.: Eur. Polym. J. *6*, 51 (1970).
7. Ferry J. D.: *Viscoelastic Properties of Polymers*. Wiley, New York 1970; Doi M., Edwards S. F.: *The Theory of Polymer Dynamics*. Clarendon Press, Oxford 1986.
8. Stockmayer W. H.: J. Chem. Phys. *17*, 588 (1949).
9. Koningsveld R., Staverman A. J.: J. Polym. Sci., A2 *6*, 305, 325, 349 (1968).
10. Koningsveld R., Staverman A. J.: Kolloid Z. Z. Polym. *218*, 114 (1967); *220*, 31 (1967).
11. Šolc K.: Macromolecules *3*, 665 (1970).
12. Šolc K., Kleintjens L. A., Koningsveld R.: Macromolecules *17*, 573 (1984).
13. Koningsveld R.: Adv. Polym. Sci. *7*, 1 (1970).
14. Rehage G., Möller D., Ernst O.: Makromol. Chem. *88*, 232 (1965).
15. Koningsveld R.: Adv. Colloid Interface Sci. *2*, 151 (1968).
16. Scholte Th. G.: J. Polym. Sci., A2 *9*, 1553 (1971).
17. Staverman A. J., Van Santen J. H.: Rec. Trav. Chim. Pays-Bas *60*, 76 (1941).
18. Staverman A. J.: Rec. Trav. Chim. Pays-Bas *60*, 640 (1941).
19. Huggins M. L.: J. Chem. Phys. *9*, 440 (1941).
20. Huggins M. L.: Ann. N. Y. Acad. Sci. *43*, 1 (1942).
21. Flory P. J.: J. Chem. Phys. *9*, 660 (1941); *10*, 51 (1942); *12*, 425 (1944).
22. Boyer R. F.: J. Polym. Sci. *8*, 73 (1952); *9*, 197 (1952).
23. Koningsveld R.: *Ph.D. Thesis*. Leiden 1967.
24. Tompa H.: Trans. Faraday Soc. *45*, 1142 (1949).
25. Koningsveld R., Staverman A. J.: J. Polym. Sci., C *16*, 1775 (1967).
26. Gordon M., Kleintjens L. A., Ready B. W., Torkington J. A.: Br. Polym. J. *10*, 170 (1978).
27. Onclin M. H., Kleintjens L. A., Koningsveld R.: Makromol. Chem., Suppl. *3*, 197 (1979).
28. Vandeweerdt P.: *Ph.D. Thesis*. Leuven 1993.
29. Šolc K.: Macromolecules *8*, 819 (1975); *10*, 1101 (1977).